ORIGINAL ARTICLE

Optimization of Spanlastic Nanovesicles for Intranasal Delivery of Fexofenadine HCl: *In vitro* and *Ex vivo* Studies

V. Yadav[1,2#], N. S. Lakshmi Priya[1,2#], Shivakumar H. Nanjappa[1,2], S. Kokila[3], Sanjana S. Prakash[1,2], S. M. Monisha[1,2], Rushikesh Shinde[1,2], K. K. Nisarga[1,2]

[1]Department of Pharmaceutics, Centre of Innovative Science and Engineering Education, KLE College of Pharmacy, Bengaluru, Karnataka, India, [2]KLE Academy of Higher Education and Research, Deemed-to-be-University, Belagavi, Karnataka, India, [3]Department of Pharmaceutics, College of Pharmacy, JSS University, Noida, Uttar Pradesh, India

[#]First author: Equal contribution

Abstract

Introduction: Fexofenadine hydrochloride (FEX), a BCS Class IV antihistamine, imparts low oral bioavailability because of its low water solubility, limited permeability, and P-glycoprotein–mediated efflux, resulting in delayed therapeutic action in allergic rhinitis (AR). **Materials and Methods:** To provide controlled drug release and improve FEX absorption, the current study set out to develop and optimize an intranasal spanlastic nanovesicular system. Ethanol injection was used to create FEX-loaded spanlastics, which were then optimized with the help of a Box–Behnken design and a quality-by-design methodology. Cumulative drug release and entrapment efficiency (%EE) were systematically assessed in relation to surfactant concentration and sonication time. **Results:** The optimized spanlastic formulation exhibited high EE (88.30 ± 2.20%) and sustained drug release (80.54 ± 2.16% in 8 h), closely matching predicted values. It showed nanoscale vesicle size (178.7 nm), good stability (−28.03 mV), and uniform distribution. Zero-order release kinetics and significantly enhanced *ex vivo* nasal permeation compared to FEX solution were observed. **Discussion:** The experimental and predicted values confirm the robustness of the optimization model. Nanoscale size and adequate zeta potential indicate suitability for intranasal delivery. Enhanced permeation is attributed to vesicle deformability and surfactant synergy, whereas refrigerated stability supports formulation reliability. **Conclusion:** The optimized spanlastic system represents a promising and patient-friendly intranasal delivery platform for improving the bioavailability and therapeutic performance of FEX in AR.

Key words: Allergic rhinitis, box–behnken, *ex vivo* permeation study, fexofenadine hydrochloride, spanlastics

INTRODUCTION

Allergic rhinitis (AR) is a highly prevalent chronic inflammatory disorder of the nasal mucosa, identified by symptoms such as rhinorrhea, sneezing, itching, and nasal congestion.[1] It affects approximately 10–30% of the global population and significantly impairs quality of life, sleep, and work productivity. The condition involves IgE-mediated hypersensitivity to environmental allergens, leading to mast cell activation and release of histamine and other inflammatory mediators.[2] Despite the availability of effective pharmacotherapy, optimal management of AR remains challenging due to limitations associated with conventional drug delivery systems.[3]

Fexofenadine hydrochloride (FEX), a second-generation selective peripheral H_1-receptor antagonist, is widely used in the management of AR and chronic idiopathic urticaria because of its favorable safety profile, minimal sedative potential, and absence of anticholinergic effects.[4] However,

Address for correspondence:
Dr. Shivakumar H. Nanjappa, Department of Pharmaceutics, KLE College of Pharmacy, Bengaluru, Karnataka, India. Off: +91-80-23325611, Fax: +91-80-23425373, Mobile: +91-9448241420.
E-mail: shivakumarhn@gmail.com

Received: 18-02-2026
Revised: 23-03-2026
Accepted: 30-03-2026

FEX, belonging to the BCS Class IV drug, is characterized by poor aqueous solubility and low permeability. Consequently, it exhibits limited oral bioavailability (~33%), mainly due to incomplete gastrointestinal absorption and P-glycoprotein–mediated efflux, along with a delayed onset of action and food-dependent variability in absorption, which may adversely affect therapeutic efficacy and patient compliance.[5]

Intranasal drug delivery has emerged as a promising alternative for AR management, offering rapid onset of action, enhanced local drug concentration at the site of action, and avoidance of hepatic first-pass metabolism.[6] The nasal cavity offers a large absorptive surface area, rich vascularization, and relatively high epithelial permeability, which would facilitate efficient drug absorption.[7] However, conventional intranasal formulations such as solutions are prone to rapid clearance by mucociliary action, limiting nasal residence time to approximately 15–20 min and reducing drug absorption and hampering the therapeutic effectiveness.[8]

To overcome these limitations, nanovesicular delivery systems such as spanlastics have gained increasing attention for intranasal applications. Spanlastics are elastic nanovesicles composed of non-ionic surfactants, wherein S60 acts as the vesicle-forming surfactant while Tween 80 functions as an edge activator, imparting membrane flexibility and deformability.[9] The incorporation of T80 disrupts the rigid bilayer structure of S60, thereby enhancing vesicle fluidity and facilitating improved penetration across the nasal epithelium. Encapsulation of FEX within spanlastic vesicles is therefore expected to enhance intranasal absorption, improve local delivery to histamine H_1 receptor sites, enable rapid onset of action, and reduce systemic exposure-related adverse effects.[10] In this context, the present study represents the first systematic effort to develop and optimize FEX-loaded spanlastic vesicles for intranasal delivery by a quality-by-design approach. A Box–Behnken design (BBD) was employed to systematically evaluate the effects of Span 60 concentration, Tween 80 concentration, and sonication time on critical quality attributes, including entrapment efficiency (EE) and cumulative drug release (CDR). This study, which aims to develop a robust intranasal formulation, is novel and first-of-its-kind for FEX, as no such study has been undertaken for the drug to the best of our knowledge.

MATERIALS AND METHODS

FEX was purchased from Dham Tec Pharma and Consultants, Mumbai, India. Span 60 was purchased from Sigma-Aldrich, Karnataka, India. Tween 80, ethanol, and sodium dihydrogen orthophosphate were purchased from S D Fine-Chem Ltd, Mumbai, India. Sodium chloride was purchased from Molychem, Mumbai, India. Sodium bicarbonate and sodium hydroxide were purchased from LobaChemie Pvt Ltd, Mumbai, India, and calcium chloride was purchased from Nice chemicals Pvt Ltd, Mumbai, India.

Preparation of spanlastics

Design of experiment (DOE)

The ishikawa (fishbone) diagram shown in Figure 1 illustrates the potential factors influencing the critical quality attributes of FEX-loaded spanlastics, identified through Failure Mode and Effects Analysis (FMEA). The development of spanlastics was undertaken after conducting a series of preliminary trials aimed at achieving optimal vesicle stability, uniformity, and reproducible entrapment of FEX. Later, a BBD was employed using Design-Expert® software (version 13.0.5.0, Stat-Ease Inc., Minneapolis, USA) to optimize the processing parameters affecting the critical quality attributes of spanlastics and thereby develop FEX-loaded spanlastics.[11]

Three independent variables were identified that were found to influence the vesicle formation and performance, which included the amount of Span 60 (125–225 mg; X_1), the amount of Tween 80 (25–125 mg; X_2), and sonication time (3–5 min; X_3). Each factor was studied at three levels, generating 17 experimental runs in a randomized order using a quadratic model without blocking. The impact of these variables on EE (Y_1) and %CDR (Y_2) was systematically evaluated to optimize and develop a robust intranasal spanlastic delivery system.[12]

Spanlastics were prepared using the ethanol injection method. Briefly, FEX and Span 60 were dissolved in ethanol (5 mL) to obtain the organic phase. The organic solution was then slowly injected into a pre-heated aqueous phase (5 mL) containing Tween 80 as an edge activator under continuous magnetic stirring using a digital magnetic stirrer (Remi Instruments Ltd., Mumbai, India) maintained at a controlled temperature to facilitate ethanol evaporation and vesicle formation. Stirring was continued to ensure uniform dispersion, and dispersion was subsequently subjected to ultrasonication using an ultrasonic water bath (GT Sonic Professional Ultrasonic Bath, Shenzhen, China) for 3–5 min to reduce vesicle size and obtain a homogeneous nanoscale spanlastic system. After sonication, the dispersion was filtered through Whatman filter paper to remove unencapsulated drug and large aggregates (Figure 2). The collected filtrate, containing spanlastic vesicles, was used for subsequent characterization.

Regression analysis

The targeted responses, %EE (Y_1) and %CDR at 8 h (Y_2) of FEX-loaded spanlastic vesicles, were statistically evaluated using analysis of variance (ANOVA) at a significance level of $P < 0.05$ with Design-Expert® software (version 13.0.5.0, Stat-Ease Inc., Minneapolis, USA). Polynomial equations (Equation 1) were generated for each response following model selection based on F-test analysis of the studied variables.

$$Y = \beta_0 + \beta_1 A + \beta_2 B + \beta_3 C + \beta_{12} AB + \beta_{13} AC + \beta_{23} BC + \beta_{11} A^2 + \beta_{22} B^2 + \beta_{33} C^2 \quad (1)$$

Where Y represents the response; β_0 is the intercept; β_1, β_2, and β_3 denote the coefficients of the linear effects; β_{12}, β_{13} and β_{23}

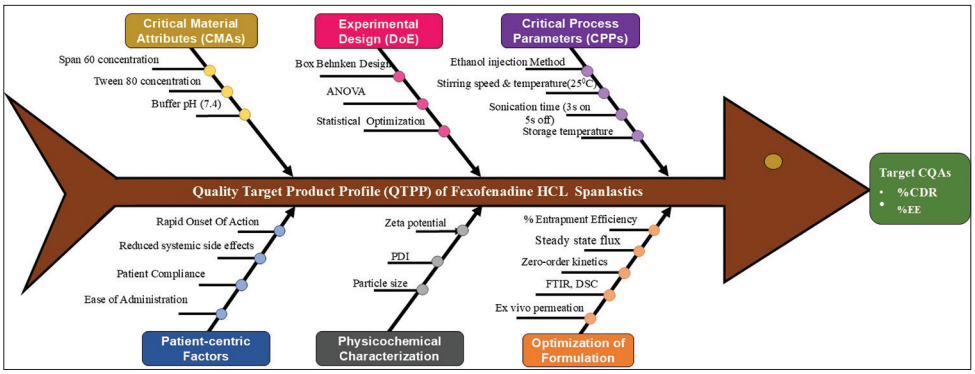

Figure 1: Fishbone diagram representing the Box–Behnken design-driven risk assessment for the development of fexofenadine HCl-loaded spanlastics

represent interaction effects, and β_{11}, β_{22}, and β_{33} correspond to quadratic effects of the independent variables. *A*, *B*, and *C* denote the amount of S60, T80, and ST, respectively. Statistically insignificant terms ($P > 0.05$) were eliminated using a backward elimination approach to obtain reduced, significant regression models. The optimized models were used to construct 3D response surfaces and contour plots to elucidate the individual and combined effects of formulation variables. The BBD comprised 16 experimental with center points of 4 runs within predefined factor ranges shown in Table 1, and the corresponding formulation compositions are presented in Table 2.

Table 1: Box–Behnken design to develop fexofenadine spanlastics

Independent variables	Low level	High level
A: S60[a] (%w/v)	2.5	4,5
B: T80[b] (%w/v)	0.5	2.5
C: ST[c] (min)	3	5
Dependent variables	Constraints set	
Y_1: Entrapment efficiency (%)	Maximize	
Y_2: CDR at 8h (%)	Maximize	

[a]Span 60; [b]Tween 80; [c]Sonication time

Optimization of formulation

The study aimed to optimize formulation and process parameters to develop FEX-loaded spanlastic vesicles with desirable critical quality attributes, namely high EE and enhanced CDR, essential for effective intranasal antihistaminic therapy. The process was optimized by a desirability function approach to validate the quadratic models, establish a design space, and identify optimal formulation conditions. Constraints were applied to maximize the drug encapsulation and ensure complete release, enabling the development of a robust and reproducible intranasal spanlastic delivery system.

Validation of the mathematical models

By creating an optimized FEX-loaded spanlastic formulation with the most desired critical quality attributes, the generated quadratic models were verified. Table 1 displays the constraints used to determine the ideal configurations with the goal of maximizing percentage %EE and %CDR. The aforementioned constraints were used to create the optimized formulation, which was then assessed for the chosen responses. To further confirm its suitability for intranasal delivery, the optimized spanlastic formulation was then put through a thorough physicochemical characterization.[13]

Evaluation of Spanlastics

Determination of percentage EE

The %EE of FEX-loaded spanlastics was determined using an indirect centrifugation method. The freshly prepared dispersion was centrifuged at 15,000 rpm for 20 min at 4°C using a refrigerated microcentrifuge (Eltek RC 4815 F, Elektrocraft Pvt. Ltd., Mumbai, India). After centrifugation, the clear supernatant containing unentrapped drug was collected, diluted appropriately with distilled water, and analyzed spectrophotometrically at 219 nm (UV-1900i, Shimadzu, Kyoto, Japan). All determinations were carried out in triplicate to ensure reproducibility. The %EE was calculated using Equation 2:[14]

$$EE(\%) = \frac{Total\ drug - free\ drug}{Total\ drug} \times 100 \quad (2)$$

Drug release studies

%CDR of spanlastics (S1–S16) and FEX were performed in a dialysis bag diffusion technique. The dialysis membrane containing the formulation was immersed in 500 *mL* of phosphate buffer (*pH* 7.4), and the study was carried out using a USP dissolution apparatus *type* II (Electrolab TDT-08L, Mumbai, India). The dissolution medium was maintained at 37 ± 0.5°C with constant stirring. The samples were withdrawn at stipulated time intervals till 8 *h*, and then swapped out for an equivalent amount of brand-new buffer kept at the same temperature. A UV-visible spectrophotometer set at 219 *nm* was used to evaluate the extracted samples after they had been appropriately diluted. Plotting the CDR(%) of medication released over time was done.[15,16]

Table 2: Composition of the model formulations of spanlastics as per Box–Behnken design

Run	S60[a](%w/v)	T80[b](%w/v)	ST[c] (min)
SF1	3.5	2.5	3
SF2	4.5	0.5	5
SF3	2.5	2.5	4
SF4	2.5	1.5	5
SF5	3.5	2.5	4
SF6	3.5	1.5	4
SF7	3.5	1.5	4
SF8	3.5	1.5	5
SF9	2.5	0.5	4
SF10	4.5	1.5	4
SF11	4.5	2.5	3
SF12	4.5	0.5	4
SF13	3.5	2.5	3
SF14	2.5	0.5	4
SF15	3.5	0.5	4
SF16	3.5	1.5	5

[a]Span60; [b]Tween 80; [c]Sonication time

Characterization of the FEX-loaded spanlastics

Compatibility studies

FTIR spectra of FEX, the physical mixture of drug and excipients, and the optimized FEX-loaded spanlastics were recorded using an FTIR spectrometer (Jasco FTIR-460 Plus, Tokyo, Japan). The samples were thoroughly mixed with spectroscopic-grade potassium bromide (KBr), loaded into a diffuse reflectance sampler, and exposed to infrared radiation. Spectral scanning was carried out over the wavenumber range of 400–4,000 cm^{-1} after running a KBr blank to identify the characteristic peaks of the drug. The spectra obtained for the physical mixture and spanlastic formulation were compared with those of FEX to assess any possible drug–excipient interactions.[17]

Measurement of particle size, polydispersity index, and zeta potential

Particle size (PS), Polydispersity Index (PDI), and Zeta potential (ZP) of spanlastics were evaluated using Zetasizer Nano ZS (Malvern Instruments Ltd., Worcestershire, UK). To attain the ideal scattering intensity, the formulations were appropriately diluted with deionized water before measurement. To ensure accuracy and reproducibility, measurements were made in triplicate, and all analyses were carried out at 25 ± 0.5°C. The following equation was used to determine each batch's EE.[18,19]

$$EE(\%) = \frac{Total\ drug - free\ drug}{Total\ drug} \times 100 \quad (3)$$

Kinetics of drug release

Attempts were made to fit the *in vitro* dissolution data of the optimized formulation, which were analyzed with the help of different kinetic models, including first order, zero-order, Korsmeyer–Peppas, and Higuchi models, to understand the kinetics and mechanism of drug release. The release model exhibiting the highest correlation coefficient (R^2) was considered to best describe the dominant drug release behavior of the formulation.[19]

Permeation study using nasal mucosa

Drug permeation of FEX from the optimized spanlastic formulation was evaluated using sheep nasal mucosa. The isolated tissue was washed, equilibrated in simulated nasal fluid (SNF, pH 7.4), and mounted on a Franz diffusion cell with the epithelial side facing the donor compartment. The receptor chamber was filled with SNF (pH 7.4) and maintained at 34 ± 1°C under constant stirring to simulate nasal conditions.

A formulation equivalent to 1 mg of FEX HCl was placed in the donor compartment. Samples (1 mL) were withdrawn from the receptor compartment at predetermined intervals over 8 h and replaced with fresh SNF to maintain sink conditions. Drug content was analyzed spectrophotometrically at 219 nm, and steady-state flux (Jss) was calculated using Equation 4.

$$J_{ss} = \frac{\Delta Qt}{\Delta t \times S} \quad (4)$$

Where ΔQt is the cumulative amount of drug permeated over time Δt, and S = 0.785 cm^2 is the effective surface area of the nasal mucosa.[20,21]

Stability studies

The stability of the optimized formulation was evaluated for 3 months by storing samples under refrigerated (4 ± 2°C) and room temperature (25 ± 2°C) conditions. Formulations were packed in airtight amber containers and analyzed at 0, 1, 2, and 3-month intervals. At each sampling point, the withdrawn samples were inspected visually for clarity, phase separation, or precipitation, followed by determination of %EE and %CDR using the previously established analytical procedures. All assessments were performed in triplicate, and the results were compared with initial values to assess physicochemical stability during storage.[22]

Analysis of statistics

Design-Expert® software version 13.0.5.0 (Minneapolis, MN, USA) was used to set up the experimental design and statistically analyze the findings. The statistical significance was defined as a $P < 0.05$.

RESULTS

Preparation of spanlastics

DOE

The BBD effectively facilitated the optimization of FEX-loaded spanlastics by evaluating the influence of S60 (X_1), T80 (X_2), and ST (X_3) on %EE (Y_1) and %CDR (Y_2). All 16 formulations prepared exhibited smooth, uniform dispersions with no signs of aggregation or phase separation. S60 played a crucial role in vesicle formation and contributed to improved EE, whereas T80 functioned as an edge activator and enhanced membrane elasticity, thereby promoting drug release. Table 1 presents the experimental runs and establishes the formulation responses.

Evaluation of spanlastics

Impact on EE

The mathematical model to illustrate the influence of different independent variables on %EE can be represented by Equation 4. The %EE of the spanlastics was found to range from 74.98 ± 0.1 to 87.99 ± 0.3% formulation S1–S16 as indicated in Table 3.

$$Y_1 = +87.99 - 1.17A - 3.33B - 0.9200C - 2.24AB + 0.4150AC + 2.15BC - 7.72A^2 - 5.55B - 6.04C \quad (5)$$

The model F-value of 6.39 indicated that the developed equation for EE was statistically significant ($P < 0.0001$). The very low probability value obtained from the Fisher F-test further confirmed the strong significance of the predictive model. The coefficient of determination ($R^2 = 0.9056$) and the adjusted R^2 (0.7639) were in reasonable agreement, with a difference of <0.2, demonstrating an adequate model fit. Moreover, refinement of the model by eliminating non-significant terms improved the adjusted R^2, bringing it closer to unity and indicating enhanced predictive accuracy.

Table 3: Experimental %EE and %CDR release of spanlastic formulation runs

Run	%EE	%CDR
SF1	74.98±0.16	67.09±0.32
SF2	82.06±0.52	76.17±0.62
SF3	71.87±0.24	63.98±0.52
SF4	76.54±0.32	68.65±0.52
SF5	76.98±0.44	67.09±0.34
SF6	73.54±0.86	67.65±0.82
SF7	87.97±0.52	80.3±0.12
SF8	80.12±0.22	71.23±0.60
SF9	74.32±0.52	69.43±0.52
SF10	65.09±0.42	58.1±0.42
SF11	72.76±0.24	66.87±0.36
SF12	73.32±0.44	68.43±0.14
SF13	87.99±0.32	80.3±0.52
SF14	79.87±0.72	72.98±0.42
SF15	88.02±2.32	80.5±0.24
SF16	87.99±0.3	80.2±0.42

%EE: Entrapment efficiency, %CDR: Cumulative drug release

The regression model indicated a negative effect of S60 (A), T80 (B), and ST (C) on %EE, as reflected by the negative coefficients of the linear terms, with Tween 80 showing the most pronounced influence. The significant negative quadratic terms confirmed a curvature response, implying reduced %EE at higher levels of the variables beyond the optimum. The %EE was found to range from 65.09 ± 0.42 to 88.04 ± 2.32. The higher %EE noted may be attributed to the lipophilic nature of FEX, which has a log p of ~ 3[23]. The concentration of Tween 80 was found to have a maximum negative effect among the three variables. An increased level of Tween 80 is likely to reduce the surface tension and therefore the spanlastic size. The smaller size would invariably result in higher amounts of surface drug and lower %EE. However, further increase in the Tween 80 concentration was found to render the spanlastics more flexible, reducing the %EE.

As shown in the contour plot [Figure 3a], the maximum %EE was observed at intermediate concentrations of S60 and T80, with a decline toward the edge of the design space. The 3D surface plot [Figure 3b] further supported this trend, displaying a peak at the central experimental domain and a reduction at extreme concentrations. The predicted versus actual plot [Figure 3c] demonstrated a close alignment of data points along the diagonal line, indicating good agreement between experimental and model-predicted %EE values and confirming the adequacy and reliability of the regression model. Overall, an optimized balance of S60 and T80, along with controlled sonication time, was found to be critical in achieving maximum EE, which correlates well with the predictive response surface model.

Impact on CDR

The mathematical model to illustrate the influence of different independent variables on EE can be represented by Equation 5. The %CDR of the spanlastics was found to range from 67.09 ± 0.1 to 80.2 ± 0.3% shown in Table 3.

$$Y_2 = 80.32 - 0.68A - 3.97B - 0.54C - 2.27AB - 0.58AC + 0.89BC - 6.22A^2 - 6.30B^2 - 5.76C^2 \quad (6)$$

The model developed for %CDR was statistically significant, as evidenced by an F-value of 6.33 with a corresponding $P<0.0001$, confirming the reliability of the regression equation. The Fisher's test further supported model significance, with $P_{model} > F < 0.0001$, indicating a minimal likelihood that the observed relationship occurred due to random variation.

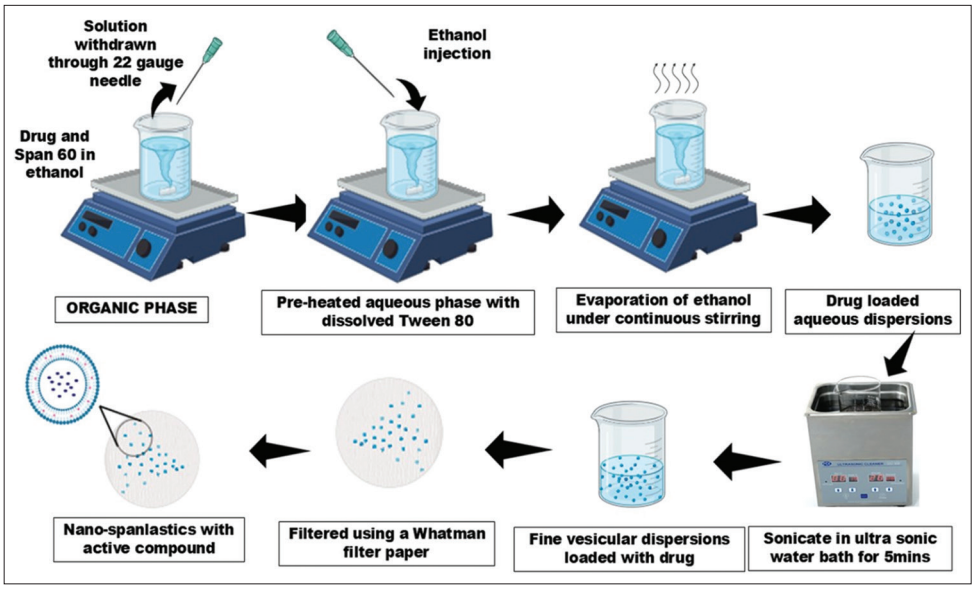

AQ6 **Figure 2:** Schematic illustration of the preparation process of spanlastics

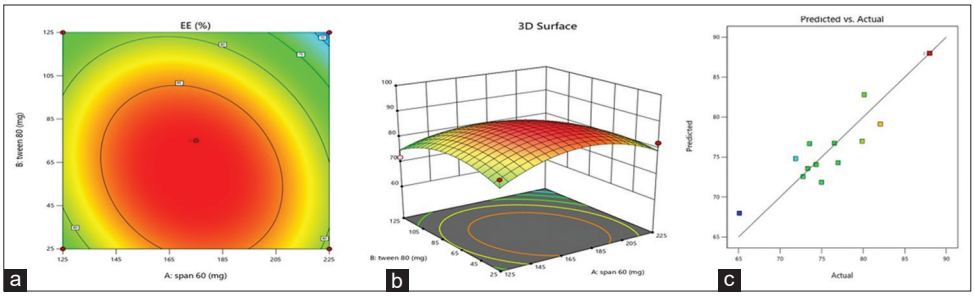

Figure 3: Graphical presentation of contour (a) and 3D Plot (b), and predicted versus actual graph showing the effect of independent variables on %entrapment efficiency

The coefficient of determination ($R^2 = 0.9047$) showed good agreement with the adjusted R^2 (0.7617), with a difference of <0.2, demonstrating adequate model fitting and minimal variation between predicted and experimental values. The improvement in adjusted R^2 after removal of non-significant terms suggests that model refinement enhanced prediction accuracy and overall robustness.

The contour plot [Figure 4a] revealed a distinct high-response region at the central levels of S60 and T80, indicating maximum %CDR within the optimized concentration range. A decline in %CDR at higher span 80 levels indicates that drug release is highly sensitive to formulation composition, with deviations from the optimum reducing diffusion through the vesicular matrix.

The 3D response surface plot [Figure 4b] corroborated this pattern, showing maximum drug release at intermediate levels of S60 and T80, with a decline at extreme concentrations of either component. Overall, the surface plots highlight that an optimal balance between S60 and T80 is essential for maximizing %CDR, reflecting a clear curvature in the response and validating the reliability of the model-predicted design space for spanlastic formulations. In addition, the predicted versus actual plot [Figure 4c] showed that the experimental %CDR values were closely clustered around the regression line, indicating strong agreement between observed and predicted responses and confirming the adequacy and predictive reliability of the developed model.

Only the terms with statistical significance ($P < 0.05$) are included in the models.

Optimization of formulation

A desirability-based numerical optimization approach was employed to determine the optimal composition of FEX-loaded spanlastic vesicles with targeted CQAs. The regression analysis confirmed that the developed quadratic models were statistically significant for both %EE (Y_1) and %CDR (Y_2), as evidenced by high R^2 and adjusted R^2 values [Table 4]. The fitted polynomial equations describing the influence of formulation variables on the responses are presented above. The optimized formulation, selected based on the maximum overall desirability value, was prepared and experimentally evaluated. The experimental %EE and %CDR values showed close agreement with the predicted values, with <2% prediction error [Table 5], validating the accuracy and

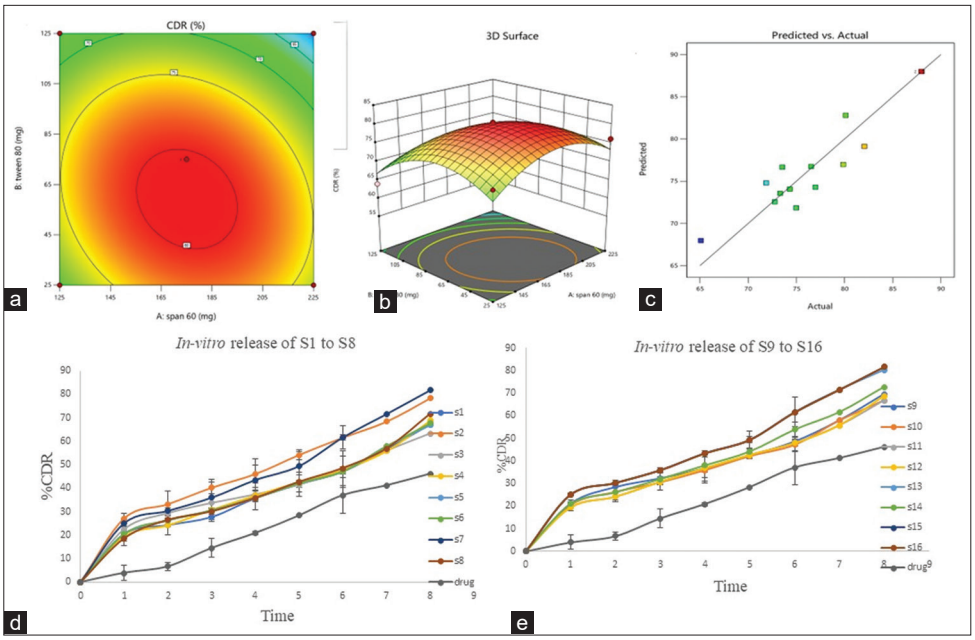

Figure 4: Graphical presentation of contour (a) and 3D Plot (b) predicted versus actual plots (3) showing the effect of independent variables on %cumulative drug release (%CDR). (%)CDR versus time (h) for formulation fexofenadine hydrochloride (FEX), S1 to S8 in (d) and FEX, S9 to S16 in (e)

reliability of the optimization model. The desirability plot [Figure 5] illustrates the region of highest overall desirability within the design space, identifying the optimal combination of S60 and T80 concentrations that simultaneously satisfies the set criteria for both responses. These findings confirm that the optimization strategy successfully identified a robust intranasal spanlastic formulation with reproducible performance for FEX delivery.

Characterization of the FEX HCl-loaded spanlastics

Compatibility studies

The FTIR spectrum of pure FEX exhibited characteristic absorption peaks at 3297.68 cm^{-1} (-OH stretching), 2992.98 cm^{-1} (-CH_2 stretching), and 1707.66 cm^{-1} (C=O stretching), confirming its structural identity. The physical mixture displayed similar peaks at 3487.54 cm^{-1}, 2921.78 cm^{-1}, and 1707.66 cm^{-1}, indicating preservation of drug functional groups in the presence of excipients. The optimized formulation also retained the corresponding bands at 3567.55 cm^{-1}, 2989.99 cm^{-1}, and 1787.89 cm^{-1}, with slight shifts observed, suggesting no significant interaction between drug and excipients. The persistence of all major characteristic peaks confirms the compatibility of FEX within the excipients used [Table 6].

Measurement of particle size, polydispersity index, and zeta potential

The optimized FEX-loaded spanlastic formulation demonstrated desirable nanoscale vesicular characteristics. The formulation exhibited an average particle size of 178.7 nm [Figure 7a], confirming successful nanoscale vesicle formation suitable for intranasal administration. The formulation displayed a PDI of 1.0, indicating a uniform and monodisperse vesicle population. The small vesicular size is expected to enhance intimate contact with the nasal mucosa, thereby facilitating direct local delivery of the drug at the nasal site rather than systemic exposure. The intensity-based size distribution graph showed a single sharp peak, further confirming vesicle homogeneity. The zeta potential value of −28.03 mV indicated good electrostatic stability of the spanlastic vesicles, as shown in Figure 7b. Collectively, these findings demonstrate that the optimized spanlastic formulation possesses suitable physicochemical attributes for effective local intranasal delivery of FEX.

Table 4: Results of regression analysis and polynomial coefficients pertaining to each critical parameter attribute

Responses	F-value	*P*-value	R^2	Adjusted R^2
Y1	6.39	<0.0001	0.9056	0.7639
Y2	6.33	<0.0001	0.9047	0.7617

Kinetics of drug release

The *in vitro* drug release data of all formulations (S1–S16) were subjected to kinetic modeling using zero-order, Higuchi, and Korsmeyer–Peppas equations to determine the overall release behavior. Based on the comparative evaluation of correlation coefficients (R^2), the zero-order kinetic model was found to best describe the drug release profile overall, indicating a constant and controlled release of drug from the formulations over time, as displayed in Table 7. The zero-order model showed good

Table 5: Composition of the optimized formulations and comparison of the experimental values of the response parameters/product quality attributes with the predicted values

Run	Optimal settings A: B: C	Responses	Experimental value	Predicted value	Percentage prediction error
17	A: S60 (%w/v) B: T80 (%w/v) C: ST (min)	Y_1 (%)	88.30±2.20	89.2	1.026
		Y_2 (%)	80.54±2.16	81.5	1.191

Table 6: Fourier transform infrared characteristics band of FEX, mixture of drug and excipients, and formulation

Vibrational band (cm^{-1})	Groups present	Observed band (cm^{-1})		
		FEX	Physical mixture	Spanlastic formulation
3200–3600	-OH (stretching)	3297.68	3487.54	3567.55
2850–3000	$-CH_2$ (stretching vibration)	2992.98	2921.78	2989.99
1600–1800	C=0 (stretching vibration)	1707.66	1707.66	1787.89

FEX: Fexofenadine hydrochloride

Table 7: Release kinetic of the developed formulations

Batch	Higuchi plot		Korsmeyer–Peppas plot			Zero order	
	*K_H (h)	R^2	n'value	*K_p (h)	R^2	Percentage h^{-1}	R^2
S1	11.61±0.03	0.9406±0.02	0.5696±0.04	0.2053±0.01	0.9546±0.01	4.10625±0.04	0.9465±0.003
S2	7.68±0.02	0.9885±0.04	0.4788±0.03	0.3438±0.03	0.9345±0.02	2.71625±0.01	0.9898±0.004
S3	12.95±0.02	0.9891±0.00	0.4003±0.02	0.4095±0.01	0.9978±0.01	4.58±0.02	0.9876±0.005
S4	11.03±0.01	0.9498±0.06	0.5903±0.04	0.2719±0.05	0.9345±0.01	3.90125±0.03	0.9556\±0.006
S5	11.73±0.02	0.9676±0.04	0.5522±0.02	0.2878±0.03	0.9789±0.03	4.1475±0.03	0.9998±0.007
S6	11.43±0.04	0.9343±0.04	0.5549±0.03	0.3040±0.01	0.9966±0.02	4.04375±0.02	0.9898±0.008
S7	6.45±0.02	0.9587±0.03	0.5726±0.01	0.2948±0.03	0.9765±0.02	2.28375±0.02	0.9456±0.009
S8	10.05±0.02	0.9742±0.02	0.606±0.02	0.2702±0.02	0.9897±0.04	3.55375±0.05	0.9989±0.010
S9	10.73±0.01	0.9876±0.01	0.3941±0.04	0.4119±0.02	0.9908±0.05	3.79625±0.03	0.9087±0.011
S10	11.73±0.04	0.9657±0.01	0.5522±0.05	0.2907±0.05	0.9765±0.06	4.1475±0.04	0.9544±0.012
S11	11.71±0.05	0.9234±0.01	0.491±0.01	0.3237±0.02	0.9432±0.07	4.14125±0.02	0.9675±0.013
S12	11.03±0.02	0.9988±0.01	0.6667±0.03	0.2201±0.01	0.9123±0.08	3.90125±0.03	0.9323±0.014
S13	6.95±0.04	0.9765±0.01	0.6667±0.05	0.2155±0.03	0.9089±0.09	2.46±0.02	0.9980±0.015
S14	11.61±0.03	0.9406±0.02	0.5696±0.04	0.2053±0.01	0.9546±0.01	4.10625±0.04	0.9465±0.003
S15	7.68±0.02	0.9885±0.04	0.4788±0.03	0.3438±0.03	0.9345±0.02	2.71625±0.01	0.9898±0.004
S16	12.95±0.02	0.9891±0.00	0.4003±0.02	0.4095±0.01	0.9978±0.01	4.58±0.02	0.9876±0.005

linearity for most formulations, with R^2 values ranging from 0.9323 to 0. 9998. The zero-order release rate constants ranged from 2.28 to 4.58% h^{-1}, reflecting formulation-dependent variations while maintaining a uniform and controlled drug release throughout the study period.

The permeation study conducted using sheep nasal mucosa demonstrated that the optimized spanlastic formulation resulted in a CDR of 531.94 ± 0.22 μg/cm^2 in 8 h that was significantly higher ($P < 0.05$) than that from FEX solution (354.18 ± 0.12 μg/cm^2). The steady-state flux (Jss) from the spanlastics was found to be 84.72 μg/h/cm^2. The enhanced permeation performance can be primarily attributed to the nanoscale vesicle size (~178.7 nm) and the synergistic roles of the incorporated non-ionic surfactants. Tween 80, acting as an edge activator, enhances vesicle elasticity and increases membrane fluidity, thereby facilitating paracellular transport across the nasal epithelium. In contrast, span 60, characterized by a low HLB value, promotes strong interactions with lipid membranes and enhances mucosal adhesion. Furthermore, the high deformability of spanlastic vesicles significantly contributes to their permeation efficiency, enabling them to traverse narrow intercellular pathways without structural disruption. Collectively, these attributes promote enhanced drug diffusion and support sustained and efficient transport across the nasal epithelial barriers shown in Figure 8.

Stability studies

A 3-month stability study was conducted to assess the optimized spanlastic formulation stored at 4 ± 2°C and 25 ± 2°C.

Monthly evaluations of %EE and %CDR indicated consistent performance under refrigerated conditions. While minor reductions were noted at room temperature, the formulation retained its functional properties throughout the study. These results confirm that the spanlastic formulation exhibits better stability when stored under refrigeration, maintaining its %EE and %CDR profile over the test period as shown in Table 8.

DISCUSSION

Fexofenadine (FEX), a BCS Class IV drug, is characterized by low aqueous solubility and poor permeability, low intestinal permeability, and P-glycoprotein–mediated efflux, leading to limited oral bioavailability and delayed onset of action.[24] To address these limitations, spanlastics – elastic surfactant-based vesicular carriers – were explored for their ability to enhance drug solubilization and controlled release to enable regional delivery to the nasal mucosa. The selected FEX dose was based on its therapeutic requirement and safety profile, with adjustment for intranasal administration to achieve effective plasma levels at a reduced dose.[25] The intranasal route was chosen to bypass hepatic first-pass metabolism and intestinal efflux mechanisms, enabling direct delivery to the H1 receptors in the nasal mucosa and faster onset of action.[26] Thus, the development of FEX-loaded spanlastic vesicles for intranasal delivery is justified to improve regional delivery, ensure rapid therapeutic response, and enhance patient compliance.

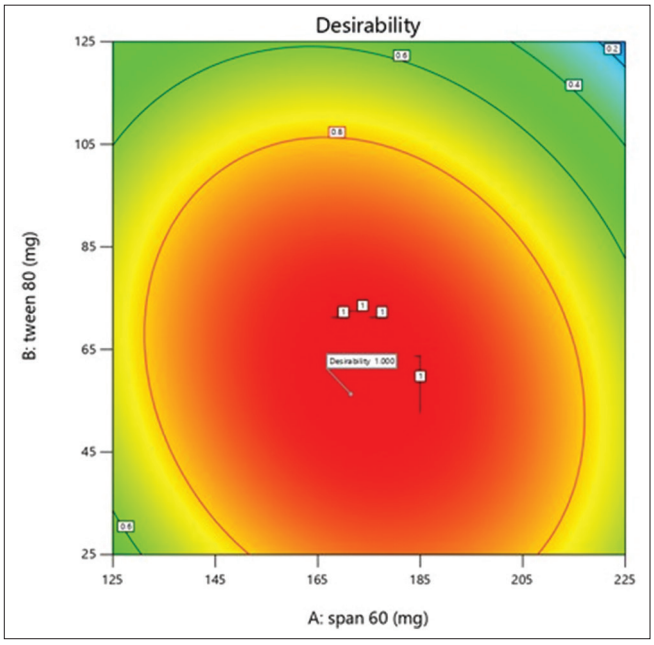

Figure 5: Desirability contour plot showing the combined effect of S60 and T80 on overall desirability, highlighting a central high-desirability region

Preparation of spanlastics

DOE

The optimization of FEX-loaded spanlastic formulations was performed using a Box–Behnken experimental design, allowing a systematic assessment of the effects of key formulation and process variables, namely the concentrations of S60 and T80, along with sonication time, on EE and CDR.[27] All the developed formulations exhibited good physical stability and uniform dispersion, indicating the suitability of the selected excipients and the adopted preparation method. S60 was selected as the primary vesicle-forming surfactant owing to its high phase transition temperature and rigid bilayer-forming ability, which contributed to improved vesicle formation and enhanced drug entrapment.[28] T80 was included as an edge activator to enhance membrane elasticity, thereby improving vesicle deformability and facilitating drug release. ST was identified as a critical process parameter, where increased sonication

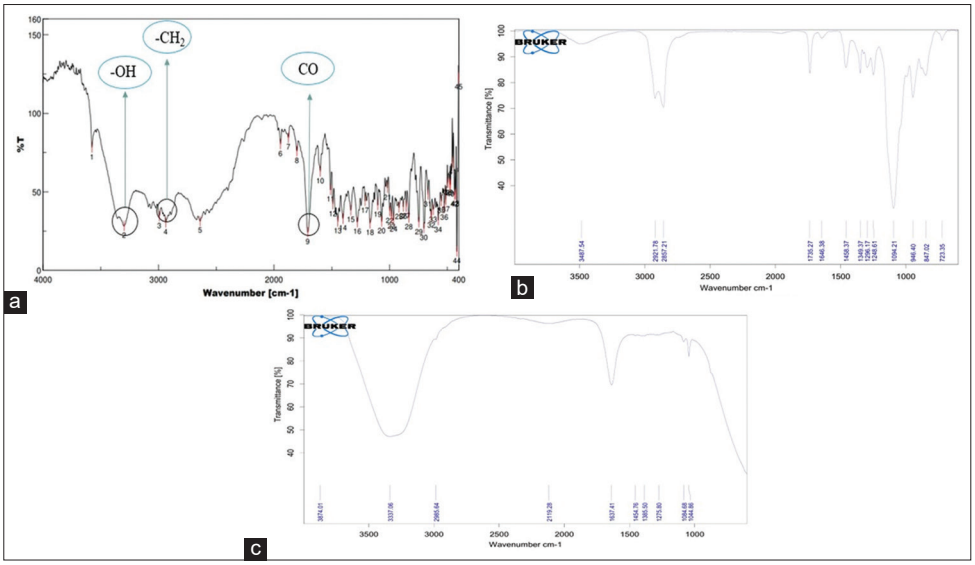

Figure 6: Fourier transform infrared spectroscopy of fexofenadine hydrochloride (a), physical mixture (b), spanlastics formulation (c)

Table 8: Percentage EE (%) and CDR (%) of the optimized formulation under different conditions

Sl. No.	Days	%EE		%CDR	
		4±2°C	25±2°C	4±2°C	25±2°C
1	0	87.99±0.15	87.99±0.14	78.27±0.11	78.27±0.16
2	30	87.99±0.11	83.25±0.14	78.03±0.18	74.24±0.19
3	60	86.4±0.18	79.16±0.19	77.38±0.15	70.51±0.13
4	90	85.92±0.11	76±0.17	76.8±0.11	65.63±0.11

%EE: Entrapment efficiency, %CDR: Cumulative drug release

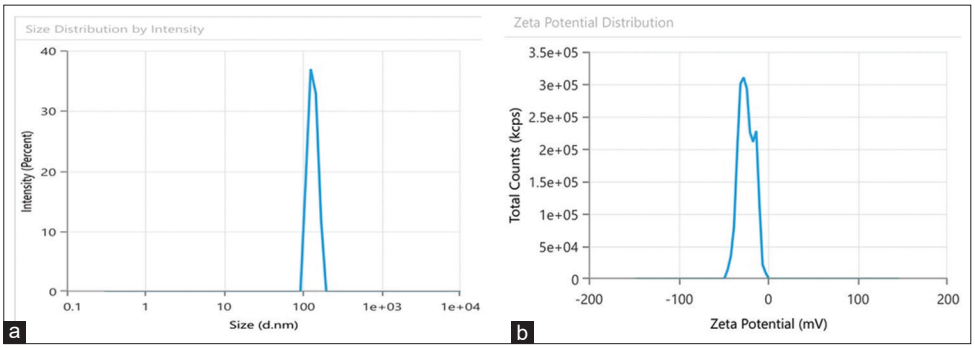

Figure 7: Particle size (a) and Zeta potential (b) of optimized formulation

led to reduced vesicle size, resulting in improved drug permeation and release characteristics.[29]

Evaluation of formulated spanlastics

Impact on %EE

The EE(%) of the FEX-loaded spanlastic formulations ranged from 74.98 ± 0.1% to 87.99 ± 0.3% for formulations as presented in Table 4. The EE of the developed spanlastic formulations was markedly influenced by the combined effect of formulation composition and processing conditions. The statistical model demonstrated a satisfactory fit, confirming its reliability in describing the experimental data and predicting formulation behavior within the design space.

Among the investigated variables, the surfactant system played a critical role in modulating drug entrapment. Higher levels of T80 exerted a comparatively stronger influence on %EE, which can be attributed to increased membrane fluidity at elevated concentrations, leading to partial drug leakage from the vesicular core. Similarly, excessive amounts of T80 and prolonged sonication were found to adversely affect entrapment, likely due to disruption of vesicular integrity and reduced bilayer stability.[30]

Response surface and contour analysis revealed that optimal entrapment was achieved within the central region of the experimental domain, indicating that moderate concentrations of both surfactants combined with controlled sonication favor efficient drug incorporation. This behavior underscores the importance of maintaining an optimal balance between vesicle rigidity and elasticity to maximize drug loading.[31]

Overall, the findings highlight that careful optimization of formulation and process variables is essential to achieve high EE in spanlastic systems, supporting their suitability for effective intranasal drug delivery.

Impact on %CDR

The %CDR of the spanlastic formulations ranged from 67.09 ± 0.1% to 80.2 ± 0.3%. The %CDR from the developed spanlastic formulations was markedly influenced by the combined effect of formulation and process variables. The release pattern suggests that vesicular membrane characteristics play a crucial role in governing drug diffusion, which is directly affected by the surfactant composition and sonication conditions. The factors were found to have a negative effect on %CDR; particularly, the concentration of T80 exhibited the most predominant negative effect, as evident from Equation 5. This predominant effect can be attributed to the ability of T80 to render the spanlastic vesicles more elastic, which may lead to drug leakage and consequently influence drug release behavior. Higher levels of surfactants, especially T80, were associated with a decline in drug release, possibly due to excessive membrane fluidization and disruption of vesicular structure, thereby restricting controlled drug diffusion.[32] In addition, at higher S60 levels, the drug is likely to become well integrated within the lipid matrix; the lipophilic nature of FEX may therefore be a primary factor contributing to the reduced drug release observed at elevated span concentrations. In contrast, intermediate concentrations of S60 and T80 promoted a favorable balance between membrane rigidity and elasticity, facilitating efficient drug release while maintaining vesicle integrity.[32] The non-linear relationship observed between the

independent variables and %CDR highlights the presence of a curvature effect, indicating a curvilinear relationship between the factors and responses. Deviation from this optimal range, either by increasing or decreasing surfactant levels, adversely affected drug release performance.[33] Overall, these findings emphasise the necessity of precise optimization of surfactant ratios and processing parameters to achieve reproducible and efficient drug release from spanlastic vesicles, reinforcing their suitability as a promising carrier system for intranasal drug delivery.

Optimization of formulation

A desirability-based numerical optimization approach was employed to determine the optimal formulation variables of FEX-loaded spanlastic vesicles with the desired critical quality attributes. Feasibility analysis and numerical optimization were carried out to obtain a formulation that simultaneously maximized %EE (Y_1) and %CDR (Y_2). The optimized spanlastic formulation, obtained at the predicted optimal levels of S60, T80, and sonication time, was subsequently prepared and experimentally evaluated. The experimentally determined values of %EE and %CDR were compared with the corresponding values predicted by the developed mathematical models, and the results are summarized in Table 5. The low prediction error observed for %EE and %CDR (<2%) confirmed the close agreement between predicted and experimental responses. These findings validate the reliability and strong predictive capability of the quadratic polynomial regression models supported by ANOVA, demonstrating the robustness of the optimization strategy for the development of FEX-loaded spanlastic vesicles.[34]

The FTIR spectrum of pure FEX displayed distinct absorption peaks corresponding to its functional groups, confirming the drug's structural integrity. A broad band at 3297.68 cm^{-1} was assigned to –OH stretching, the peak at 2992.98 cm^{-1} to $–CH_2$ stretching, and the signal at 1707.66 cm^{-1} to C=O stretching vibrations. These findings are consistent with previously reported spectral data, verifying the authenticity of the drug.

The physical mixture exhibited all major characteristic peaks of FEX with only slight positional shifts, suggesting the absence of chemical interaction with the selected excipients. Likewise, the optimized spanlastic formulation preserved the essential FEX absorption bands with minor shifts, likely due to physical interactions or hydrogen bonding rather than chemical incompatibility.[35]

Measurement of PS, PDI, and ZP

The optimized FEX-loaded spanlastic formulation exhibited a mean PS of 178.7 nm, an index PDI of 1.0, and a ZP of −28.03 mV, indicating successful development of a nanoscale vesicular system. The particle size within the nanometric range is considered optimal for intranasal delivery, as such vesicles can efficiently interact with the nasal epithelium and enhance permeation across the olfactory mucosa, thereby facilitating direct nose-to-brain transport while minimizing systemic exposure. The PDI value reflects a uniform vesicle population, suggesting consistency in the formulation process and homogeneity in vesicle size distribution, which is essential for reproducible drug delivery performance. The negative zeta potential value of −28.03 mV indicates sufficient electrostatic repulsion between vesicles, contributing to improved colloidal stability by preventing aggregation. Overall, the combination of appropriate particle size, uniform size distribution, and adequate surface charge confirms that the optimised spanlastic formulation possesses the required physicochemical attributes for stable and effective intranasal delivery of FEX.[36]

Kinetics of drug release

The drug release profiles of the spanlastic formulations (S1–S16) showed the highest correlation with the zero-order kinetic model, as evidenced by the regression analysis. By high correlation coefficients [R^2 = 0.9323–0.9998; Table 7]. The zero-order release rate constants (k_0) ranged from 2.28 to 4.58 % h^{-1}, reflecting formulation-dependent variations while maintaining a consistent and uniform drug release pattern over the study duration.[37] The prevalence of zero-order kinetics indicates that drug release from the spanlastic vesicles occurred at a constant rate, independent of drug concentration. This release behavior can be ascribed to the structured vesicular bilayer of spanlastics, which serves as a diffusion-controlling barrier by uniformly entrapping the drug within the surfactant matrix. The rigid bilayer contributed by S60, in combination with the elasticity imparted by T80, facilitates regulated and sustained drug diffusion.[38] Moreover, the nanoscale size and homogeneous distribution of vesicles ensure uniform surface area exposure, further supporting concentration-independent release kinetics.[39] Collectively, the observed zero-order release pattern highlights the capability of the developed spanlastic system to provide controlled and predictable drug delivery, which is particularly beneficial for intranasal administration by sustaining drug availability at the absorption site and potentially improving therapeutic outcomes.[40]

The *ex vivo* permeation study across sheep nasal mucosa demonstrated that the optimized FEX-loaded spanlastic formulation achieved a cumulative drug permeation of 531.94 µg/cm^2 within 8 h, with a corresponding steady-state flux (Jss) of 84.72 µg/h/cm^2 [Figure 6]. These values indicate a markedly enhanced and sustained permeation profile, confirming the efficiency of the developed spanlastic system for intranasal delivery. The high permeation performance can be primarily attributed to the nanoscale vesicle size (~178.7 nm), which enables close contact with the nasal epithelium and facilitates diffusion through the mucosal barrier. The presence of T80 as an edge activator increases vesicle elasticity and membrane fluidity, thereby enhancing paracellular transport across the tight junctions of the nasal mucosa.[41] In addition, S60, owing to its low HLB value, promotes stronger interactions with the lipid components

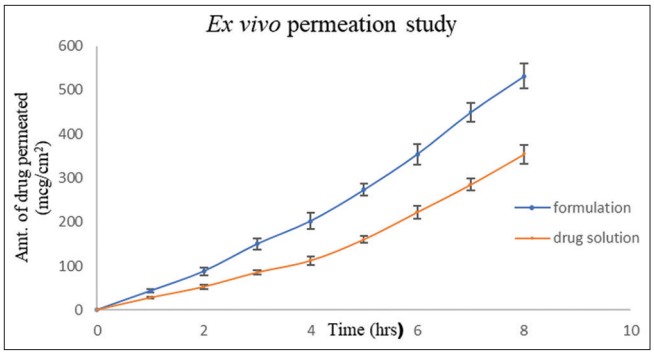

Figure 8: Fexofenadine hydrochloride HCl *ex vivo* permeation from the spanlastic optimized formula

of the nasal membrane, improving vesicle adhesion and residence time at the absorption site.[42] Furthermore, the high deformability of spanlastic vesicles allows them to traverse narrow intercellular pathways without loss of structural integrity, which significantly contributes to the observed high flux and cumulative permeation.[43] Collectively, these formulation attributes synergistically enhance drug diffusion and support sustained transport across the nasal epithelial barrier, substantiating the suitability of the optimized spanlastic formulation for efficient intranasal delivery of FEX.

The stability studies demonstrated that the optimized spanlastic formulation remained stable over 3 months, with superior performance observed under refrigerated storage (4 ± 2°C). The consistent EE and drug release under these conditions can be attributed to reduced bilayer fluidity and minimized vesicle fusion or drug leakage at lower temperatures.[44] Although minor reductions in %EE and %CDR were observed at room temperature (25 ± 2°C), the formulation retained its functional integrity throughout the study period. Overall, these findings indicate that the spanlastic system is physically stable, with refrigeration providing optimal storage conditions to preserve vesicular integrity and formulation performance.[45]

CONCLUSION

This study successfully formulated and optimized FEX-loaded spanlastic vesicles as a potential intranasal delivery platform to address the poor oral bioavailability of FEX. Application of the BBD allowed systematic evaluation and optimization of critical formulation and process variables, yielding a formulation with high EE, controlled CDR, and strong model predictability, as evidenced by minimal prediction error. The optimized spanlastics exhibited nanosized vesicles with satisfactory colloidal stability, followed by zero-order release kinetics, and showed no chemical incompatibility between the drug and excipients. Furthermore, enhanced and sustained *ex vivo* permeation across sheep nasal mucosa confirmed the effectiveness of the deformable spanlastic system in enabling direct drug delivery through the nasal mucosal membrane. Stability studies demonstrated good formulation stability, particularly under refrigerated conditions. Collectively, these results validate the developed spanlastic vesicles as a stable and promising intranasal carrier for FEX, offering controlled release and enhanced permeation, and warrant further *in vivo* evaluation for clinical translation.

AUTHOR CONTRIBUTIONS

Conceptualization: Shivakumar H. N., Lakshmi Priya N.S, Yadav V. Software: Yadav V, Monisha S.M, Sanjana S Prakash, Rushikesh Shinde. Data curation: Lakshmi Priya N.S, Shivakumar H. N., Yadav V. Formal analysis: Yadav V, Sanjana S Prakash, Kokila S. Investigation: Lakshmi Priya N.S. Methodology: Lakshmi Priya N.S. Project administration: Lakshmi Priya N.S. Resources: Lakshmi Priya N.S., Shivakumar H. N. Validation: Shivakumar H.N. Visualization: Yadav V, Sanjana S Prakash, Monisha S.M, Nisarga K.K., Rushikesh Shinde. Supervision: Shivakumar H.N. Writing-original draft: Yadav V., Monisha S.M., Nisarga KK. Writing-review and editing: Yadav V, Sanjana S Prakash, Kokila S., and Rushikesh Shinde. All authors have read and agreed to the published version of the manuscript.

ACKNOWLEDGMENT

The authors are also grateful to Vision Group of Science and Technology, Bengaluru, Karnataka, India, for providing the necessary equipment needed to undertake the research work.

REFERENCES

1. Terada T, Kawata R. Diagnosis and treatment of local allergic rhinitis. Pathogens 2022;11:80.
2. Zhang Y, Lan F, Zhang L. Update on pathomechanisms and treatments in allergic rhinitis. Allergy 2022;77:3309-19.
3. Klimek L, Mullol J, Ellis AK, Izquierdo-Domínguez A, Hagemann J, Casper I, *et al*. Current management of allergic rhinitis. J Allergy Clin Immunol Pract 2024;12:1399-412.
4. Song WY, Han CS, Yu WS, Jang JW, Kim GW, Jeon YS, *et al*. Formulation and bioequivalence evaluation of a miniaturized fexofenadine hydrochloride tablet. Pharmaceutics 2025;17:756.
5. Abdelhameed AH, Abdelhafez WA, Hamad AA, Mohamed MS. Formulation and optimization of oral fast dissolving films loaded with nanosuspension to enhance the oral bioavailability of Fexofenadine HCL. J Drug Deliv Sci Technol 2023;85:104578.
6. Lombardo R, Musumeci T, Carbone C, Pignatello R. Nanotechnologies for intranasal drug delivery: An update of literature. Pharm Dev Technol 2021;26:824-45.
7. Fortuna A, Schindowski K, Sonvico F. Intranasal drug

delivery: Challenges and opportunities. Front Pharmacol 2022;13:868986.
8. Wu X, Zang R, Qiu Y, Zhang Y, Peng J, Cheng Z, *et al*. Intranasal drug delivery technology in the treatment of central nervous system diseases: Challenges, advances, and future research directions. Pharmaceutics 2025;17:775.
9. Saini H, Rapolu Y, Razdan K, Nirmala SV. Spanlastics: A novel elastic drug delivery system with potential applications via multifarious routes of administration. J Drug Target 2023;31:999-1012.
10. Alharbi WS, Hareeri RH, Bazuhair M, Alfaleh MA, Alhakamy NA, Fahmy UA, *et al*. Spanlastics as a potential platform for enhancing the brain delivery of flibanserin: *In vitro* response-surface optimization and *in vivo* pharmacokinetics assessment. Pharmaceutics 2022;14:2627.
11. Ansari MD, Saifi Z, Pandit J, Khan I, Solanki P, Sultana Y, *et al*. Spanlastics a novel nanovesicular carrier: Its potential application and emerging trends in therapeutic delivery. AAPS PharmSciTech 2022;23:112.
12. Ibrahim SS, Abd-Allah H. Spanlastic nanovesicles for enhanced ocular delivery of vanillic acid: Design, *in vitro* characterization, and *in vivo* anti-inflammatory evaluation. Int J Pharm 2022;625:122068.
13. Dahash RA, Ghareeb MM. Design, development, and optimization of spanlastics for delivery of rizatriptan benzoate. Iraqi J Pharm Sci 2025;34:125-40.
14. Shukr MH, Ismail S, El-Hossary GG, El-Shazly AH. Spanlastics nanovesicular ocular insert as a novel ocular delivery of travoprost: Optimization using Box-Behnken design and *in vivo* evaluation. J Liposome Res 2022;32:354-64.
15. Eedara BB, Nyavanandi D, Narala S, Veerareddy PR, Bandari S. Improved dissolution rate and intestinal absorption of fexofenadine hydrochloride by the preparation of solid dispersions: *In vitro* and *in situ* evaluation. Pharmaceutics 2021;13:310.
16. Alaaeldin E, Mostafa M, Mansour HF, Soliman GM. Spanlastics as an efficient delivery system for the enhancement of thymoquinone anticancer efficacy: Fabrication and cytotoxic studies against breast cancer cell lines. J Drug Deliv Sci Technol 2021;65:102725.
17. Wagdi MA, Salama A, El-Liethy MA, Shalaby ES. Comparative study of niosomes and spanlastics as a promising approach for enhancing benzalkonium chloride topical wound healing: *In-vitro* and *in-vivo* studies. J Drug Deliv Sci Technol 2023;84:104456.
18. Aziz D, Mohamed SA, Tayel S, Makhlouf A. Enhanced ocular anti-aspergillus activity of tolnaftate employing novel cosolvent-modified spanlastics: Formulation, statistical optimization, kill kinetics, *ex vivo* trans-corneal permeation, *in vivo* histopathological and susceptibility study. Pharmaceutics 2022;14:1746.
19. Ibrahim MS, Elkady OA, Amer MA, Noshi SH. Exploiting response surface D-optimal design study for preparation and optimization of spanlastics loaded with miconazole nitrate as a model antifungal drug for topical application. J Pharm Innov 2023;18:2402-18.
20. Singh B, Saini G, Vyas M, Verma S, Thakur S. Optimized chronomodulated dual release bilayer tablets of fexofenadine and montelukast: Quality by design, development, and *in vitro* evaluation. Future J Pharm Sci 2019;5:5.
21. Nasr AM, Qushawy MK, Elkhoudary MM, Gawish AY, Elhady SS, Swidan SA. Quality by design for the development and analysis of enhanced *in-situ* forming vesicles for the improvement of the bioavailability of fexofenadine HCl *in vitro* and *in vivo*. Pharmaceutics 2020;12:409.
22. Elbasuony AR, Abdelaziz AE, Mazyed EA, El Maghraby GM. Niosomes for enhanced oral delivery of pioglitazone: *In vitro* characterization and *in vivo* evaluation. J Pharm Pharmacol 2025;77:1075-84.
23. Elnaggar MG, Mekkawy AI, Taha AF, Abdel-Maksoud FM, Elnaggar MG, Tawfeek HM, *et al*. Mizolastine-loaded spanlastics for treatment of atopic dermatitis: Immunomodulatory approach for management of inflammation. J Drug Target 2025:1-11.
24. Türkmen Ö, Şenyiğit ZA, Baloğlu E. Formulation and evaluation of fexofenadine hydrochloride orally disintegrating tablets for pediatric use. J Drug Delivery Sci Technol 2018;43:201-10.
25. Ahmed S, Nazmi M, Hasan I, Sultana S, Haldar S, Reza MS. Fexofenadine HCl immediate release tablets: *in vitro* characterization and evaluation of excipients. Bangladesh Pharma J. 2013;16:1-9
26. Abdelhameed AH, Abdelhafez WA, Saleh KH, Mohamed MS. Formulation, optimization, and *in-vivo* evaluation of nanostructured lipid carriers loaded with Fexofenadine HCL for oral delivery. J Drug Deliv Sci Technol 2022;74:103607.
27. Xu D, Song XJ, Chen X, Wang JW, Cui YL. Advances and future perspectives of intranasal drug delivery: A scientometric review. J Control Release 2024;367:366-84.
28. Seary H, Barakat EH, Raslan MA, Samy AM. Development, characterization, and optimization of repaglinide loaded spanlastics along with investigation of drug solubility in various media. Univers J Pharm Res 2024;9:105-12.
29. Quintanar-Guerrero D, Zambrano-Zaragoza MD, Gutiérrez-Cortez E, Mendoza-Muñoz N. Impact of the emulsification-diffusion method on the development of pharmaceutical nanoparticles. Recent Pat Drug Deliv Formul 2012;6:184-94.
30. Saitoh H, Takami K, Ohnari H, Chiba Y, Ikeuchi-Takahashi Y, Obata Y. Effects and mode of action of oleic acid and tween 80 on skin permeation of disulfiram. Chem Pharm Bull 2023;71:289-98.
31. Owodeha-Ashaka K, Ilomuanya MO, Iyire A. Evaluation of sonication on stability-indicating properties of optimized pilocarpine hydrochloride-loaded niosomes in ocular drug delivery. Prog Biomater 2021;10:207-20.

32. Pornputtapitak W, Thiangjit Y, Tantirungrotechai Y. Effect of functional groups in lipid molecules on the stability of nanostructured lipid carriers: Experimental and computational investigations. ACS Omega 2024;9:11012-24.
33. Unnisa A, Chettupalli AK, Al Hagbani T, Khalid M, Jandrajupalli SB, Chandolu S, *et al*. Development of dapagliflozin solid lipid nanoparticles as a novel carrier for oral delivery: Statistical design, optimization, *in-vitro* and *in-vivo* characterization, and evaluation. Pharmaceuticals (Basel) 2022;15:568.
34. Fatima A, Begum A, Yaseen M. Formulation and evaluation of fexofenadine nanoparticles loaded in gel. Int J Sci Res 2023;12:277-81.
35. Fatouh AM, Elshafeey AH, Abdelbary A. Liver targeting of ledipasvir via galactosylated chitosan-coated spanlastics: Chemical synthesis, statistical optimization, *in vitro*, and pharmacokinetic evaluation. Drug Deliv Transl Res 2022;12:1161-74.
36. Gautam AJ, Wairkar S. Transdermal delivery of risedronate via spanlastics for osteoporosis: formulation optimization, skin deposition, and pharmacokinetic assessment. Naunyn Schmiedebergs Arch Pharmacol 2026;399:6833-47.
37. El-Shenawy AA, Abd Elkarim RA, Mahmoud RA, Ramadan AE, Alamri AH, Abdelkader H, *et al*. Zaleplon nanospanlastics loaded transdermal patches: Formulation, optimization, *ex-vivo* permeation, and *in-vivo* studies. J Pharm Pharm Sci 2025;28:15406.
38. Alkilani AZ, Alkhaldi R, Basheer HA, Amro BI, Alhusban MA. Fabrication of thymoquinone and ascorbic acid-loaded spanlastics gel for hyperpigmentation: *In vitro* release, cytotoxicity, and skin permeation studies. Pharmaceutics 2025;17:48.
39. Priyanka S, Nithya R. Lisinopril dihydrate loaded nano-spanlastic bio-adhesive gel for intranasal delivery: 23 factorial optimization, fabrication and *ex*-vivo studies for enhanced mucosal permeation. J Res Pharm 2022;26:884-99.
40. Elkomy MH, Zaki RM, Alsaidan OA, Elmowafy M, Zafar A, Shalaby K, *et al*. Intranasal nanotransferosomal gel for quercetin brain targeting: I. Optimization, characterization, brain localization, and cytotoxic studies. Pharmaceutics 2023;15:1805.
41. Abd Elrady AN, Elkhatib MM, Mohamed MI, Fatouh AM. Spanlastics-loaded buccal films for improved olmesartan delivery and sustained hypertension management: Formulation, statistical optimization, *in vitro* and *in vivo* evaluation. J Pharma Innovation 2026;21:156.
42. Barakat EH, Kassem AM, Ibrahim MF, Elsayad MK, Abdelgawad WY, Salama A, *et al*. Fabrication of prostructured spanlastics gel for improving transdermal effect of dapagliflozin: *In vitro* characterization studies and *in vivo* antidiabetic activity. J Drug Deliv Sci Technol 2024;97:105804.
43. Seary H, Barakat EH, Raslan MA, Samy AM. Development, characterization, and optimization of repaglinide loaded spanlastics along with investigation of drug solubility in various media. Univers J Pharm Res 2024;9:105-12.
44. Sarhan FA, ElGogary R, Hamzaa MY, Soliman ME. Penetration enhancer containing vesicles for dermal and transdermal drug delivery. A review. Arch Pharm Sci Ain Shams Univ 2023;7:348-75.
45. Safhi AY, Naveen NR, Rolla KJ, Bhavani PD, Kurakula M, Hosny KM, *et al*. Enhancement of antifungal activity and transdermal delivery of 5-flucytosine via tailored spanlastic nanovesicles: statistical optimization, *in-vitro* characterization, and *in-vivo* biodistribution study. Front Pharmacol 2023;14:1321517.

Source of Support: Nil. **Conflicts of Interest:** None declared.